FERMILAB-PUB-10/409-E

Search for single vector-like quarks in $p\bar{p}$ collisions at $\sqrt{s} = 1.96$ TeV

V.M. Abazov,[35] B. Abbott,[72] B.S. Acharya,[29] M. Adams,[48] T. Adams,[46] G.D. Alexeev,[35] G. Alkhazov,[39] A. Alton[a],[60] G. Alverson,[59] G.A. Alves,[2] L.S. Ancu,[34] M. Aoki,[47] Y. Arnoud,[14] M. Arov,[57] A. Askew,[46] B. Åsman,[40] O. Atramentov,[64] C. Avila,[8] J. BackusMayes,[79] F. Badaud,[13] L. Bagby,[47] B. Baldin,[47] D.V. Bandurin,[46] S. Banerjee,[29] E. Barberis,[59] P. Baringer,[55] J. Barreto,[2] J.F. Bartlett,[47] U. Bassler,[18] V. Bazterra,[48] S. Beale,[6] A. Bean,[55] M. Begalli,[3] M. Begel,[70] C. Belanger-Champagne,[40] L. Bellantoni,[47] S.B. Beri,[27] G. Bernardi,[17] R. Bernhard,[22] I. Bertram,[41] M. Besançon,[18] R. Beuselinck,[42] V.A. Bezzubov,[38] P.C. Bhat,[47] V. Bhatnagar,[27] G. Blazey,[49] S. Blessing,[46] K. Bloom,[63] A. Boehnlein,[47] D. Boline,[69] T.A. Bolton,[56] E.E. Boos,[37] G. Borissov,[41] T. Bose,[58] A. Brandt,[75] O. Brandt,[23] R. Brock,[61] G. Brooijmans,[67] A. Bross,[47] D. Brown,[17] J. Brown,[17] X.B. Bu,[47] M. Buehler,[78] V. Buescher,[24] V. Bunichev,[37] S. Burdin[b],[41] T.H. Burnett,[79] C.P. Buszello,[40] B. Calpas,[15] E. Camacho-Pérez,[32] M.A. Carrasco-Lizarraga,[55] B.C.K. Casey,[47] H. Castilla-Valdez,[32] S. Caughron,[67] S. Chakrabarti,[69] D. Chakraborty,[49] K.M. Chan,[53] A. Chandra,[77] G. Chen,[55] S. Chevalier-Théry,[18] D.K. Cho,[74] S.W. Cho,[31] S. Choi,[31] B. Choudhary,[28] T. Christoudias,[42] S. Cihangir,[47] D. Claes,[63] J. Clutter,[55] M. Cooke,[47] W.E. Cooper,[47] M. Corcoran,[77] F. Couderc,[18] M.-C. Cousinou,[15] A. Croc,[18] D. Cutts,[74] M. Ćwiok,[30] A. Das,[44] G. Davies,[42] K. De,[75] S.J. de Jong,[34] E. De La Cruz-Burelo,[32] F. Déliot,[18] M. Demarteau,[47] R. Demina,[68] D. Denisov,[47] S.P. Denisov,[38] S. Desai,[47] K. DeVaughan,[63] H.T. Diehl,[47] M. Diesburg,[47] A. Dominguez,[63] T. Dorland,[79] A. Dubey,[28] L.V. Dudko,[37] D. Duggan,[64] A. Duperrin,[15] S. Dutt,[27] A. Dyshkant,[49] M. Eads,[63] D. Edmunds,[61] J. Ellison,[45] V.D. Elvira,[47] Y. Enari,[17] H. Evans,[51] A. Evdokimov,[70] V.N. Evdokimov,[38] G. Facini,[59] T. Ferbel,[68] F. Fiedler,[24] F. Filthaut,[34] W. Fisher,[61] H.E. Fisk,[47] M. Fortner,[49] H. Fox,[41] S. Fuess,[47] T. Gadfort,[70] A. Garcia-Bellido,[68] V. Gavrilov,[36] P. Gay,[13] W. Geist,[19] W. Geng,[15,61] D. Gerbaudo,[65] C.E. Gerber,[48] Y. Gershtein,[64] G. Ginther,[47,68] G. Golovanov,[35] A. Goussiou,[79] P.D. Grannis,[69] S. Greder,[19] H. Greenlee,[47] Z.D. Greenwood,[57] E.M. Gregores,[4] G. Grenier,[20] Ph. Gris,[13] J.-F. Grivaz,[16] A. Grohsjean,[18] S. Grünendahl,[47] M.W. Grünewald,[30] F. Guo,[69] G. Gutierrez,[47] P. Gutierrez,[72] A. Haas[c],[67] S. Hagopian,[46] J. Haley,[59] L. Han,[7] K. Harder,[43] A. Harel,[68] J.M. Hauptman,[54] J. Hays,[42] T. Head,[43] T. Hebbeker,[21] D. Hedin,[49] H. Hegab,[73] A.P. Heinson,[45] U. Heintz,[74] C. Hensel,[23] I. Heredia-De La Cruz,[32] K. Herner,[60] G. Hesketh,[59] M.D. Hildreth,[53] R. Hirosky,[78] T. Hoang,[46] J.D. Hobbs,[69] B. Hoeneisen,[12] M. Hohlfeld,[24] S. Hossain,[72] Z. Hubacek,[10,18] N. Huske,[17] V. Hynek,[10] I. Iashvili,[66] R. Illingworth,[47] A.S. Ito,[47] S. Jabeen,[74] M. Jaffré,[16] S. Jain,[66] D. Jamin,[15] R. Jesik,[42] K. Johns,[44] M. Johnson,[47] D. Johnston,[63] A. Jonckheere,[47] P. Jonsson,[42] J. Joshi,[27] A. Juste[d],[47] K. Kaadze,[56] E. Kajfasz,[15] D. Karmanov,[37] P.A. Kasper,[47] I. Katsanos,[63] R. Kehoe,[76] S. Kermiche,[15] N. Khalatyan,[47] A. Khanov,[73] A. Kharchilava,[66] Y.N. Kharzheev,[35] D. Khatidze,[74] M.H. Kirby,[50] J.M. Kohli,[27] A.V. Kozelov,[38] J. Kraus,[61] A. Kumar,[66] A. Kupco,[11] T. Kurča,[20] V.A. Kuzmin,[37] J. Kvita,[9] S. Lammers,[51] G. Landsberg,[74] P. Lebrun,[20] H.S. Lee,[31] S.W. Lee,[54] W.M. Lee,[47] J. Lellouch,[17] L. Li,[45] Q.Z. Li,[47] S.M. Lietti,[5] J.K. Lim,[31] D. Lincoln,[47] J. Linnemann,[61] V.V. Lipaev,[38] R. Lipton,[47] Y. Liu,[7] Z. Liu,[6] A. Lobodenko,[39] M. Lokajicek,[11] P. Love,[41] H.J. Lubatti,[79] R. Luna-Garcia[e],[32] A.L. Lyon,[47] A.K.A. Maciel,[2] D. Mackin,[77] R. Madar,[18] R. Magaña-Villalba,[32] S. Malik,[63] V.L. Malyshev,[35] Y. Maravin,[56] J. Martínez-Ortega,[32] R. McCarthy,[69] C.L. McGivern,[55] M.M. Meijer,[34] A. Melnitchouk,[62] D. Menezes,[49] P.G. Mercadante,[4] M. Merkin,[37] A. Meyer,[21] J. Meyer,[23] N.K. Mondal,[29] G.S. Muanza,[15] M. Mulhearn,[78] E. Nagy,[15] M. Naimuddin,[28] M. Narain,[74] R. Nayyar,[28] H.A. Neal,[60] J.P. Negret,[8] P. Neustroev,[39] S.F. Novaes,[5] T. Nunnemann,[25] G. Obrant,[39] J. Orduna,[32] N. Osman,[42] J. Osta,[53] G.J. Otero y Garzón,[1] M. Owen,[43] M. Padilla,[45] M. Pangilinan,[74] N. Parashar,[52] V. Parihar,[74] S.K. Park,[31] J. Parsons,[67] R. Partridge[c],[74] N. Parua,[51] A. Patwa,[70] B. Penning,[47] M. Perfilov,[37] K. Peters,[43] Y. Peters,[43] G. Petrillo,[68] P. Pétroff,[16] R. Piegaia,[1] J. Piper,[61] M.-A. Pleier,[70] P.L.M. Podesta-Lerma[f],[32] V.M. Podstavkov,[47] M.-E. Pol,[2] P. Polozov,[36] A.V. Popov,[38] M. Prewitt,[77] D. Price,[51] S. Protopopescu,[70] J. Qian,[60] A. Quadt,[23] B. Quinn,[62] M.S. Rangel,[2] K. Ranjan,[28] P.N. Ratoff,[41] I. Razumov,[38] P. Renkel,[76] P. Rich,[43] M. Rijssenbeek,[69] I. Ripp-Baudot,[19] F. Rizatdinova,[73] M. Rominsky,[47] C. Royon,[18] P. Rubinov,[47] R. Ruchti,[53] G. Safronov,[36] G. Sajot,[14] A. Sánchez-Hernández,[32] M.P. Sanders,[25] B. Sanghi,[47] A.S. Santos,[5] G. Savage,[47] L. Sawyer,[57] T. Scanlon,[42] R.D. Schamberger,[69] Y. Scheglov,[39] H. Schellman,[50] T. Schliephake,[26] S. Schlobohm,[79] C. Schwanenberger,[43] R. Schwienhorst,[61] J. Sekaric,[55] H. Severini,[72] E. Shabalina,[23] V. Shary,[18] A.A. Shchukin,[38] R.K. Shivpuri,[28] V. Simak,[10] V. Sirotenko,[47] P. Skubic,[72] P. Slattery,[68] D. Smirnov,[53]

K.J. Smith,[66] G.R. Snow,[63] J. Snow,[71] S. Snyder,[70] S. Söldner-Rembold,[43] L. Sonnenschein,[21] A. Sopczak,[41] M. Sosebee,[75] K. Soustruznik,[9] B. Spurlock,[75] J. Stark,[14] V. Stolin,[36] D.A. Stoyanova,[38] M. Strauss,[72] D. Strom,[48] L. Stutte,[47] L. Suter,[43] P. Svoisky,[72] M. Takahashi,[43] A. Tanasijczuk,[1] W. Taylor,[6] M. Titov,[18] V.V. Tokmenin,[35] Y.-T. Tsai,[68] D. Tsybychev,[69] B. Tuchming,[18] C. Tully,[65] P.M. Tuts,[67] L. Uvarov,[39] S. Uvarov,[39] S. Uzunyan,[49] R. Van Kooten,[51] W.M. van Leeuwen,[33] N. Varelas,[48] E.W. Varnes,[44] I.A. Vasilyev,[38] P. Verdier,[20] L.S. Vertogradov,[35] M. Verzocchi,[47] M. Vesterinen,[43] D. Vilanova,[18] P. Vint,[42] P. Vokac,[10] H.D. Wahl,[46] M.H.L.S. Wang,[68] J. Warchol,[53] G. Watts,[79] M. Wayne,[53] M. Weber[g],[47] L. Welty-Rieger,[50] A. White,[75] D. Wicke,[26] M.R.J. Williams,[41] G.W. Wilson,[55] S.J. Wimpenny,[45] M. Wobisch,[57] D.R. Wood,[59] T.R. Wyatt,[43] Y. Xie,[47] C. Xu,[60] S. Yacoob,[50] R. Yamada,[47] W.-C. Yang,[43] T. Yasuda,[47] Y.A. Yatsunenko,[35] Z. Ye,[47] H. Yin,[47] K. Yip,[70] S.W. Youn,[47] J. Yu,[75] S. Zelitch,[78] T. Zhao,[79] B. Zhou,[60] J. Zhu,[60] M. Zielinski,[68] D. Zieminska,[51] and L. Zivkovic[67]

(The D0 Collaboration*)

[1] *Universidad de Buenos Aires, Buenos Aires, Argentina*
[2] *LAFEX, Centro Brasileiro de Pesquisas Físicas, Rio de Janeiro, Brazil*
[3] *Universidade do Estado do Rio de Janeiro, Rio de Janeiro, Brazil*
[4] *Universidade Federal do ABC, Santo André, Brazil*
[5] *Instituto de Física Teórica, Universidade Estadual Paulista, São Paulo, Brazil*
[6] *Simon Fraser University, Vancouver, British Columbia, and York University, Toronto, Ontario, Canada*
[7] *University of Science and Technology of China, Hefei, People's Republic of China*
[8] *Universidad de los Andes, Bogotá, Colombia*
[9] *Charles University, Faculty of Mathematics and Physics, Center for Particle Physics, Prague, Czech Republic*
[10] *Czech Technical University in Prague, Prague, Czech Republic*
[11] *Center for Particle Physics, Institute of Physics, Academy of Sciences of the Czech Republic, Prague, Czech Republic*
[12] *Universidad San Francisco de Quito, Quito, Ecuador*
[13] *LPC, Université Blaise Pascal, CNRS/IN2P3, Clermont, France*
[14] *LPSC, Université Joseph Fourier Grenoble 1, CNRS/IN2P3, Institut National Polytechnique de Grenoble, Grenoble, France*
[15] *CPPM, Aix-Marseille Université, CNRS/IN2P3, Marseille, France*
[16] *LAL, Université Paris-Sud, CNRS/IN2P3, Orsay, France*
[17] *LPNHE, Universités Paris VI and VII, CNRS/IN2P3, Paris, France*
[18] *CEA, Irfu, SPP, Saclay, France*
[19] *IPHC, Université de Strasbourg, CNRS/IN2P3, Strasbourg, France*
[20] *IPNL, Université Lyon 1, CNRS/IN2P3, Villeurbanne, France and Université de Lyon, Lyon, France*
[21] *III. Physikalisches Institut A, RWTH Aachen University, Aachen, Germany*
[22] *Physikalisches Institut, Universität Freiburg, Freiburg, Germany*
[23] *II. Physikalisches Institut, Georg-August-Universität Göttingen, Göttingen, Germany*
[24] *Institut für Physik, Universität Mainz, Mainz, Germany*
[25] *Ludwig-Maximilians-Universität München, München, Germany*
[26] *Fachbereich Physik, Bergische Universität Wuppertal, Wuppertal, Germany*
[27] *Panjab University, Chandigarh, India*
[28] *Delhi University, Delhi, India*
[29] *Tata Institute of Fundamental Research, Mumbai, India*
[30] *University College Dublin, Dublin, Ireland*
[31] *Korea Detector Laboratory, Korea University, Seoul, Korea*
[32] *CINVESTAV, Mexico City, Mexico*
[33] *FOM-Institute NIKHEF and University of Amsterdam/NIKHEF, Amsterdam, The Netherlands*
[34] *Radboud University Nijmegen/NIKHEF, Nijmegen, The Netherlands*
[35] *Joint Institute for Nuclear Research, Dubna, Russia*
[36] *Institute for Theoretical and Experimental Physics, Moscow, Russia*
[37] *Moscow State University, Moscow, Russia*
[38] *Institute for High Energy Physics, Protvino, Russia*
[39] *Petersburg Nuclear Physics Institute, St. Petersburg, Russia*
[40] *Stockholm University, Stockholm and Uppsala University, Uppsala, Sweden*
[41] *Lancaster University, Lancaster LA1 4YB, United Kingdom*
[42] *Imperial College London, London SW7 2AZ, United Kingdom*
[43] *The University of Manchester, Manchester M13 9PL, United Kingdom*
[44] *University of Arizona, Tucson, Arizona 85721, USA*
[45] *University of California Riverside, Riverside, California 92521, USA*
[46] *Florida State University, Tallahassee, Florida 32306, USA*
[47] *Fermi National Accelerator Laboratory, Batavia, Illinois 60510, USA*

[48] University of Illinois at Chicago, Chicago, Illinois 60607, USA
[49] Northern Illinois University, DeKalb, Illinois 60115, USA
[50] Northwestern University, Evanston, Illinois 60208, USA
[51] Indiana University, Bloomington, Indiana 47405, USA
[52] Purdue University Calumet, Hammond, Indiana 46323, USA
[53] University of Notre Dame, Notre Dame, Indiana 46556, USA
[54] Iowa State University, Ames, Iowa 50011, USA
[55] University of Kansas, Lawrence, Kansas 66045, USA
[56] Kansas State University, Manhattan, Kansas 66506, USA
[57] Louisiana Tech University, Ruston, Louisiana 71272, USA
[58] Boston University, Boston, Massachusetts 02215, USA
[59] Northeastern University, Boston, Massachusetts 02115, USA
[60] University of Michigan, Ann Arbor, Michigan 48109, USA
[61] Michigan State University, East Lansing, Michigan 48824, USA
[62] University of Mississippi, University, Mississippi 38677, USA
[63] University of Nebraska, Lincoln, Nebraska 68588, USA
[64] Rutgers University, Piscataway, New Jersey 08855, USA
[65] Princeton University, Princeton, New Jersey 08544, USA
[66] State University of New York, Buffalo, New York 14260, USA
[67] Columbia University, New York, New York 10027, USA
[68] University of Rochester, Rochester, New York 14627, USA
[69] State University of New York, Stony Brook, New York 11794, USA
[70] Brookhaven National Laboratory, Upton, New York 11973, USA
[71] Langston University, Langston, Oklahoma 73050, USA
[72] University of Oklahoma, Norman, Oklahoma 73019, USA
[73] Oklahoma State University, Stillwater, Oklahoma 74078, USA
[74] Brown University, Providence, Rhode Island 02912, USA
[75] University of Texas, Arlington, Texas 76019, USA
[76] Southern Methodist University, Dallas, Texas 75275, USA
[77] Rice University, Houston, Texas 77005, USA
[78] University of Virginia, Charlottesville, Virginia 22901, USA
[79] University of Washington, Seattle, Washington 98195, USA

(Dated: December 8, 2010)

We present a search for hypothetical vector-like quarks in $p\bar{p}$ collisions at $\sqrt{s} = 1.96$ TeV. The data were collected by the D0 detector at the Fermilab Tevatron Collider and correspond to an integrated luminosity of 5.4 fb^{-1}. We select events with a final state composed of a W or Z boson and a jet consistent with a heavy object decay. We observe no significant excess in comparison to the background prediction and set limits on production cross sections for vector-like quarks decaying to W+jet and Z+jet. These are the most stringent limits to date for electroweak single vector-like quark production at hadron colliders.

PACS numbers: 12.60.-i, 13.85.Rm, 14.65.Jk

The standard model (SM) of particle physics, despite its many successes in accurately describing interactions below the TeV scale, is known to suffer shortcomings at higher energy scales. A wide range of theories have therefore been proposed to describe phenomena at the TeV scale and beyond, among them warped extra dimensions [1], universal extra dimensions [2], and little Higgs [3] models. There exist particular realizations of each of these theories that predict the existence of vector-like quarks [4–6], massive particles which share many characteristics with SM quarks. The notable exception is that the right-handed and left-handed components of vector-like quarks transform in the same way under $SU(3) \times SU(2) \times U(1)$, hence their name.

Previous searches for strong pair production of vector-like quarks at the Fermilab Tevatron Collider have excluded masses of up to 338 GeV at the 95% C.L. [7]. However, recent years have seen the development of theoretical scenarios in which corrections to SM quark couplings arising from their mixing with vector-like quarks cancel out, permitting the two types of quarks to mix to a degree unconstrained by precision electroweak measurements and b-factory results. Such large mixing with no introduction of anomalous couplings allows for single production of vector-like quarks at hadron colliders via the weak interaction [4]. Diagrams for single electroweak

*with visitors from [a]Augustana College, Sioux Falls, SD, USA, [b]The University of Liverpool, Liverpool, UK, [c]SLAC, Menlo Park, CA, USA, [d]ICREA/IFAE, Barcelona, Spain, [e]Centro de Investigacion en Computacion - IPN, Mexico City, Mexico, [f]ECFM, Universidad Autonoma de Sinaloa, Culiacán, Mexico, and [g]Universität Bern, Bern, Switzerland.

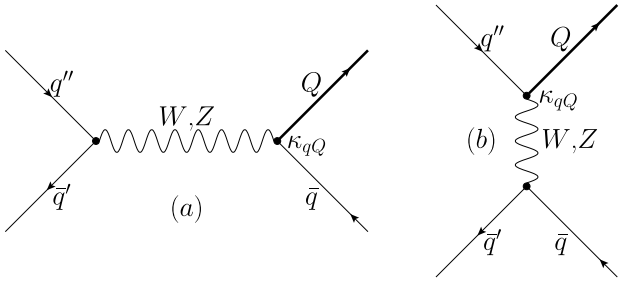

FIG. 1: s-channel (a) and t-channel (b) electroweak production of a vector-like quark Q at the Tevatron.

vector-like quark production are shown in Figure 1.

Generally, electroweak couplings to SM quarks are set by the parameter κ_{qQ}:

$$\kappa_{qQ} = \frac{v}{m_Q}\tilde{\kappa}_{qQ}, \tag{1}$$

where v is the vacuum expectation value of the SM Higgs field, m_Q is the mass of the vector-like quark, and $\tilde{\kappa}_{qQ}$ is the coupling strength. Provided this coupling is not too small, a search for singly produced vector-like quarks can benefit from the lower kinematic threshold compared to pair production and stands to improve the mass limit considerably.

In this Letter, we present a search for singly produced vector-like quarks using data corresponding to an integrated luminosity of 5.4 fb^{-1} collected by the D0 detector [8] at the Fermilab Tevatron Collider. We consider a model [4] in which there are two doublets of vector-like quarks that couple to the first generation of SM quarks. Vector-like quark final states are characterized by either a W or Z boson and at least two jets, one of which results from the decay of the vector-like quark, while another is produced in association with the vector-like quark at the primary vertex. We select events in which the vector boson decays to either electron(s) or muon(s).

The D0 detector is described in detail in [8]. The region of the D0 detector closest to the interaction point contains a central-tracking system consisting of a silicon microstrip tracker (SMT) and a central fiber tracker (CFT), both of which are located within a 2 T superconducting solenoidal magnet. Hits in these two detectors are used to reconstruct tracks from charged particles. Surrounding the two tracking subdetectors are liquid-argon and uranium calorimeters, both electromagnetic and hadronic, which have a central section (CC) covering pseudorapidities [9] $|\eta| \lesssim 1.1$, and two end calorimeters (EC) that extend coverage to $|\eta| \approx 4.2$, with all three housed in separate cryostats. Electrons are identified as isolated energy clusters in the electromagnetic calorimeter, with a shape consistent with that of an electron, matched to a track in the inner detector. Jets are reconstructed in the calorimeters using the iterative midpoint cone algorithm [10] with a cone of radius $\mathcal{R} = 0.5$ in $\eta - \phi$ space. An outer muon system, providing coverage for $|\eta| < 2$, consists of a layer of tracking detectors and scintillation trigger counters in front of 1.8 T toroids, followed by two similar layers after the toroids. Muons are identified via a combination of reconstructed tracks in both the outer muon system and the central tracking system, and are required to be isolated from both tracker and calorimeter activity.

Vector-like quark signals and background processes which include electrons or muons from W or Z boson decays are modeled using Monte Carlo (MC) simulation. Signal samples are generated using MADGRAPH [11], with CTEQ6L1 [12] parton distribution functions, LO cross sections from [4] and vector-like quark resonance widths calculated with BRIDGE [13]. Subsequent parton shower evolution is generated with PYTHIA [14]. We set $\tilde{\kappa}_{uD} = 1, \tilde{\kappa}_{uU} = \sqrt{2}$ and $\tilde{\kappa}_{dU} = \tilde{\kappa}_{dD} = 0$, such that down-type vector-like quarks decay exclusively to Wq and up-type quarks decay exclusively to Zq. This choice, while affecting the production rates and therefore the excluded vector-like quark masses, does not affect the cross section limits themselves. We generate up- and down-type vector-like quark signals with masses between 280 GeV and 700 GeV. Backgrounds from $t\bar{t}$, $W \to \ell\nu$+jets, and $Z \to \ell\ell$+jets production are modeled using ALPGEN [15], also interfaced to PYTHIA. For these events, we use a matching procedure to avoid double counting partons produced by ALPGEN and those added by the showering in PYTHIA [16]. Diboson samples are generated with PYTHIA, and single top quark production is modeled using the COMPHEP [17] generator. All MC samples are passed through a GEANT [18] simulation of the D0 detector and are overlaid with data events from randomly chosen beam crossings to simulate the effect of multiple $p\bar{p}$ interactions and detector noise. MC events are then reconstructed using the same software that is used for data reconstruction. The W+jets and Z+jets samples are normalized to the leading-log cross section reported by ALPGEN times a k-factor calculated by MCFM [19]. The $t\bar{t}$ samples are normalized to a next-to-next-to-leading order (NNLO) cross section for $m_t = 172.5$ GeV [20], and the diboson samples (WW, WZ and ZZ) to the NLO cross section predicted by MCFM [21]. All simulated events are corrected for differences in trigger and reconstruction efficiencies between data and simulation.

We conduct the search in two channels, corresponding to vector-like quark decays to ($W \to \ell\nu$)+jet and to ($Z \to \ell\ell$)+jet. In the W+jets channel, we initially select events which have passed a single lepton trigger and contain exactly one electron ($|\eta| < 1.1$) or muon ($|\eta| < 2.0$) with transverse momentum $p_T > 20$ GeV, at least two jets with $p_T > 20$ GeV and $|\eta| < 2.5$, and missing transverse energy $\not\!\!E_T$, corrected for the momentum of any muons in the event, greater than 15 GeV. We also require $2M_T^W + \not\!\!E_T > 80$ GeV, where M_T^W is the trans-

verse mass of the lepton-$\not\!\!E_T$ system, in order to suppress the multijet background. In the Z+jets channel, we initially select events with exactly two electrons or muons in addition to at least two jets, all with same p_T thresholds as used in the W+jets channel. Events are selected by a mixture of single lepton, dilepton and lepton plus jets triggers. Due to the low rate of background without real Z bosons, electrons are also accepted in the endcap electromagnetic calorimeters ($1.5 < |\eta| < 2.5$). The two leptons are required to have an invariant mass between 70 and 110 GeV, i.e. consistent with that of a Z boson. Additionally, we require $\not\!\!E_T < 50$ GeV, as this channel contains only instrumental sources of missing transverse energy.

The largest physics background to the single lepton channel is $W(\to \ell\nu)$+jets production, with smaller contributions from Z+jets, $t\bar{t}$, diboson, and single top quark processes. The main instrumental background arises from multijet events in which one of the jets is misidentified as a high-p_T isolated lepton in the detector. We model this background using data events which fail the calorimeter shower shape requirements for the electron or the isolation requirements for the muon, but pass all other selection criteria. In the single electron channel, we estimate the relative fraction of real electrons from W boson decays and misidentified electrons from jets by determining the efficiencies for each type of event to pass a tighter selection. These efficiencies are calculated in $Z \to ee$ data for real electrons and in a $\not\!\!E_T < 20$ GeV sample for misidentified electrons. In the single muon channel, we scale the events failing the muon isolation requirement to match the number of events obtained after subtracting the expected number of real W bosons satisfying the event selection from the number of events observed in data.

In the dilepton channel, $(Z \to \ell\ell)$+jets events dominate the SM background. In order to correct the Monte Carlo for the small trigger inefficiency in the data, we apply a global normalization determined using a pure $Z \to \ell\ell$ sample. The ratio between the data yield in this sample and the predicted yield from the inclusive Z boson cross section multiplied by the branching ratio is associated with the overall trigger efficiency, and the Monte Carlo distributions are scaled by this ratio. The multijet background is modeled using data events in which both leptons fail quality criteria (for electrons) or isolation criteria (for muons), and is normalized to the difference between data and MC in the dilepton mass window between 40 and 70 GeV.

The signal contains events with a W or Z boson and jets, all with high transverse momentum, as the decay products of a high mass resonance. We apply several kinematic selection criteria to select events of this type and to minimize the contributions from SM background processes. In the single lepton channel, we require lepton $p_T > 50$ GeV, highest jet $p_T > 100$ GeV, $\not\!\!E_T > 40(50)$ GeV for the muon (electron) channel, and that the separation in azimuthal angle ϕ between the lepton and the $\not\!\!E_T$ be less than 2. As the signal contains real W bosons, we additionally require $M_T^W < 150$ GeV. Finally, we exploit the relationship between the lepton charge and the η of the jet with the second-highest p_T in the signal topology. This jet, which we assign to the SM quark produced in association with the vector-like quark, is emitted, in general, into one of the forward regions of the detector, and its direction is strongly correlated with the charge of the produced vector-like quark, and thus also with the charge of the lepton from its decay. We therefore require $Q_\ell \times \eta_{j_2} > 0$, where Q_ℓ is the lepton charge and η_{j_2} is the η of the jet with the second-highest p_T in the event. This selection is efficient for the signal ($\approx 85\%$), while reducing the SM background by roughly a factor of two.

TABLE I: Predicted number of background events including total uncertainties and observed number of data events after final selection.

Process	Single lepton sample	Dilepton sample
Multijet	47.7 ± 4.7	< 0.1
Z+jets	39.9 ± 7.4	262 ± 45
W+jets	901 ± 159	0.3 ± 0.2
Top	193 ± 24	0.57 ± 0.06
Diboson	38.6 ± 3.8	8.3 ± 0.7
Background sum	1220 ± 161	271 ± 45
Data	1175	285

In the dilepton channel, we similarly select events with properties characteristic of a heavy resonance decay to a Z boson and a jet. We require the p_T of the dilepton system to be greater than 100 GeV, the spatial separation of the two leptons in $\eta - \phi$ space ($\Delta\mathcal{R}$) to be less than 2.0, and the leading jet p_T to be greater than 100 GeV.

Table I displays the observed number of data events, along with estimated background yields, after the final event selection in the single lepton and dilepton channels. Fig. 2 shows the reconstructed vector-like quark transverse mass, defined as

$$(M_T^Q)^2 = (\sqrt{p_{T_W}^2 + M_W^2} + p_{T_{j_1}})^2 - (\vec{p}_{T_W} + \vec{p}_{T_{j_1}})^2, \quad (2)$$

for the single lepton channel, where $M_W = 80.3$ GeV is the mass of the W boson and $\vec{p}_{T_{j1}}$ refers to the transverse momentum of the leading jet in the event. Also shown in Fig. 2 is the vector-like quark mass in the dilepton channel, reconstructed as the invariant mass of the dilepton + leading jet system.

Major sources of systematic uncertainty common to both analyses include modeling of W/Z+jets backgrounds (15%); cross sections for $t\bar{t}$ (10%), diboson (6%), and W/Z+jets (6%) production; and jet energy scale and resolution (1%–5%). Major systematic uncertain-

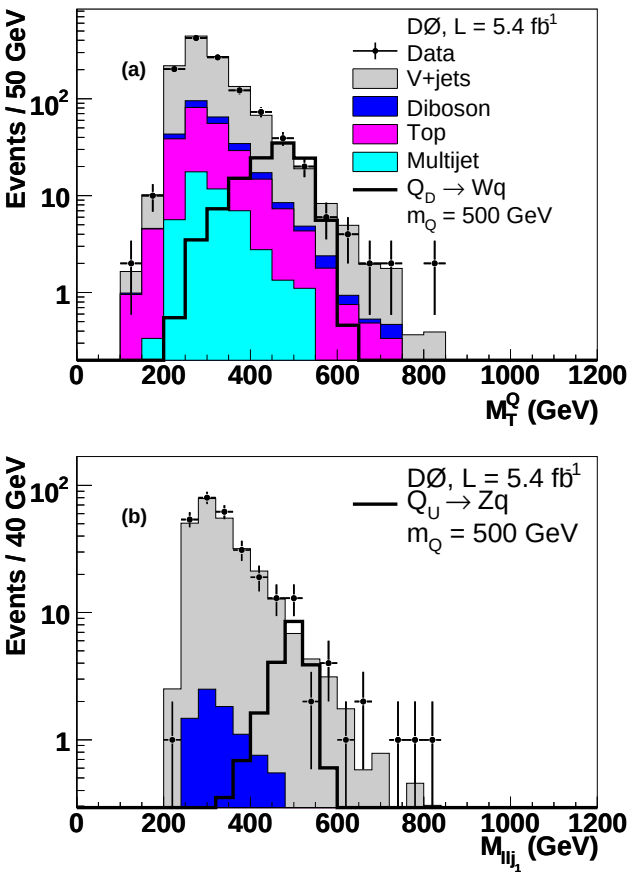

FIG. 2: (a) Vector-like quark transverse mass and (b) vector-like quark mass for the single lepton and dilepton channels, respectively. Distributions for signal processes $Q_D \rightarrow Wq$ and $Q_U \rightarrow Zq$ are normalized to the integrated luminosity of the data and include detector acceptance and reconstruction efficiencies. These assume $\tilde{\kappa}_{uD} = 1$ and $\tilde{\kappa}_{uU} = \sqrt{2}$.

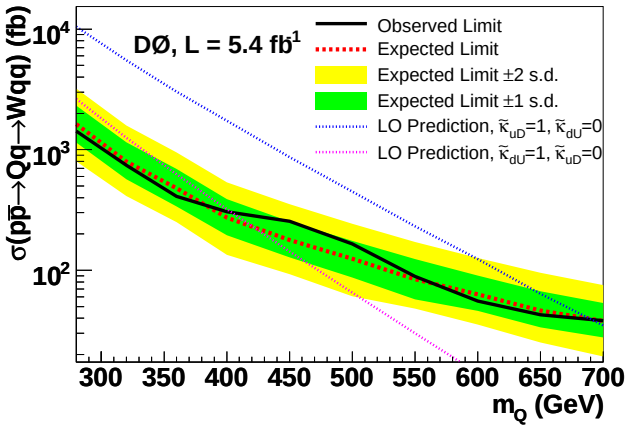

FIG. 3: Excluded production cross section for a vector-like quark Q decaying to Wq as a function of m_Q, compared to LO predictions of vector-like quark production with different $\tilde{\kappa}_{qQ}$.

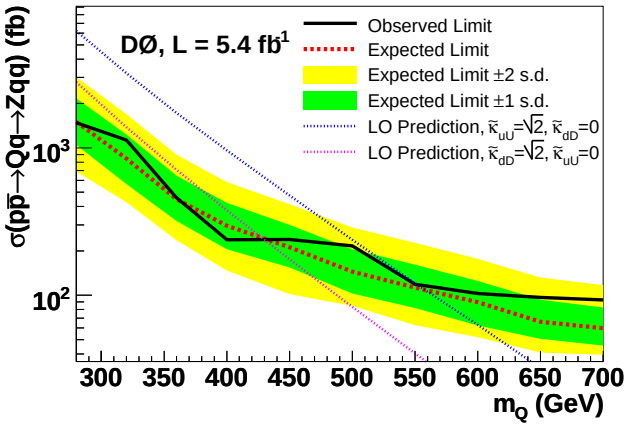

FIG. 4: Excluded production cross section for a vector-like quark Q decaying to Zq as a function of m_Q, compared to LO predictions of vector-like quark production with different $\tilde{\kappa}_{qQ}$.

ties unique to the single lepton analysis include integrated luminosity (6.1%) [22], lepton identification efficiencies (3%), high-p_T muon modeling, and trigger modeling (1%). A systematic uncertainty of 5% is assigned to the global background normalization applied to the dilepton MC samples. Systematic uncertainties on multijet normalization are 6.5%–100%, depending on the channel. These do not have a large effect on the overall background prediction, as the estimated multijet background is small after the final selection.

We observe no significant excess of data over the background prediction in either channel, therefore we set limits on vector-like quark production cross sections. We employ a modified frequentist approach using the D0 likelihood fitter [23] that incorporates a log-likelihood ratio (LLR) test statistic [24]. We calculate confidence levels for the signal plus background (CL_{s+b}) and background-only (CL_b) hypotheses by integrating the (LLR) distributions obtained by generating pseudo-experiments using Poisson statistics. Systematic uncertainties are treated as uncertainties on the expected number of signal and background events. The 95% confidence level limit is defined as the signal cross section for which $CL_s \equiv CL_{s+b}/CL_b$ is 0.05. Using as discriminant variables the vector-like quark transverse mass for decays to Wq and the vector-like quark mass for decays to Zq, we obtain 95% C.L. limits on vector-like quark production cross sections. These are shown in Figs. 3 and 4, along with leading order theoretical predictions for two different scenarios. For the case of $\tilde{\kappa}_{uD} = 1$ and $\tilde{\kappa}_{uU} = \sqrt{2}$ with no coupling to the down quark, we exclude masses below 693 GeV for a vector-like quark decaying exclusively to Wq and masses below 551 GeV for a vector-like quark decaying exclusively to Zq at the 95% C.L. For an alternate scenario defined by $\tilde{\kappa}_{dU} = 1$ and $\tilde{\kappa}_{dD} = \sqrt{2}$ with no coupling to the up quark, the corresponding mass limits are 403 GeV and 430 GeV, respectively.

In summary, we have presented a search for single vector-like quark production at the Tevatron in the W+jets and Z+jets final states. The observed data are consistent with the background expectation and limits on vector-like quark cross sections are derived. We exclude vector-like quark masses below 693 GeV for decays to Wq and masses below 551 GeV for decays to Zq at 95% C.L. assuming vector-like quark – SM quark mixing parameters $\tilde{\kappa}_{uD} = 1$ and $\tilde{\kappa}_{uU} = \sqrt{2}$ along with 100% branching ratios to the respective final states.

We thank the staffs at Fermilab and collaborating institutions, and acknowledge support from the DOE and NSF (USA); CEA and CNRS/IN2P3 (France); FASI, Rosatom and RFBR (Russia); CNPq, FAPERJ, FAPESP and FUNDUNESP (Brazil); DAE and DST (India); Colciencias (Colombia); CONACyT (Mexico); KRF and KOSEF (Korea); CONICET and UBACyT (Argentina); FOM (The Netherlands); STFC and the Royal Society (United Kingdom); MSMT and GACR (Czech Republic); CRC Program and NSERC (Canada); BMBF and DFG (Germany); SFI (Ireland); The Swedish Research Council (Sweden); and CAS and CNSF (China).

We additionally thank Marcela Carena and Anupama Atre of the Fermi National Accelerator Laboratory for providing the MADGRAPH implementation of the vector-like quarks model.

[1] L. Randall and R. Sundrum, Phys. Rev. Lett. **83**, 3370 (1999).
[2] T. Applequist, H.C. Cheng, and B.A. Dobrescu, Phys. Rev. D **64**, 035002 (2002).
[3] N. Arkani-Hamed, A.G. Cohen, E. Katz, and A.E. Nelson *et al.*, J. High Energy Phys. **07**, 034 (2002).
[4] A. Atre, M. Carena, T. Han, and J. Santiago, Phys. Rev. D **79**, 054018 (2009).
[5] K. Kong, S.C. Park, and T.G. Rizzo, J. High Energy Phys. **07**, 059 (2010).
[6] T. Han, H. Logan, B. McElrath, and L. Wang, Phys. Rev. D **67**, 095004 (2003).
[7] T. Aaltonen *et al.* (CDF Collaboration), Phys. Rev. Lett. **104**, 091801 (2010).
[8] V.M. Abazov *et al.* (D0 Collaboration), Nucl. Instrum. Methods Phys. Res. A **565**, 463 (2006).
[9] The D0 detector utilizes a right-handed coordinate system with the z axis pointing in the direction of the proton beam and the y axis pointing upwards. The azimuthal angle ϕ is defined in the x-y plane measured from the x axis. The pseudorapidity is defined as $\eta = -\ln[\tan(\theta/2)]$, where $\theta = \arctan(\sqrt{x^2+y^2}/z)$. Transverse variables are defined as projections of the variables onto the x-y plane.
[10] G.C. Blazey *et al.*, arXiv:hep-ex/005012.
[11] J. Alwall *et al.*, J. High Energy Phys. **09**, 028 (2007).
[12] J. Pumplin *et al.*, J. High Energy Phys. **07**, 012 (2002); D. Stump *et al.*, J. High Energy Phys. **10**, 046 (2003).
[13] P. Meade and M. Reese, arXiv:hep-ph/0703031.
[14] T. Sjöstrand *et al.*, Comput. Phys. Commun. **135**, 238 (2001).
[15] M.L. Mangano *et al.*, J. High Energy Phys. **07**, 001 (2003).
[16] S. Höche *et al.*, arXiv:hep-ph/0602031.
[17] E. Boos *et al.*, Nucl. Instrum. Methods Phys. Res. A **534**, 250 (2004).
[18] R. Brun and F. Carminati, CERN Program Library Long Writeup W5013, 1993 (unpublished).
[19] J. Campbell and R.K. Ellis, Phys. Rev. D **65**, 113007 (2002).
[20] S. Moch and P. Uwer, Phys. Rev. D **78**, 034003 (2008).
[21] J.M. Campbell and R.K. Ellis, Phys. Rev. D **60**, 113006 (1999).
[22] T. Andeen *et al.*, FERMILAB-TM-2365 (2007).
[23] W. Fisher, FERMILAB-TM-2386-E.
[24] T. Junk, Nucl. Instrum. Methods Phys. Res. A **434**, 435 (1999); A. Read, J. Phys. G **28** 2693 (2002).